JPhys Photonics

PAPER • OPEN ACCESS

Compact achromatic optical Fourier transform system using geometric-phase lenses

To cite this article: Ignacio Moreno *et al* 2025 *J. Phys. Photonics* **7** 045032

Journal of Physics: Photonics

PAPER

Compact achromatic optical Fourier transform system using geometric-phase lenses

Ignacio Moreno[1,2], Santiago Ríos-Álvarez[1], Pascuala García-Martínez[3,*], David Marco[4] and María del Mar Sánchez-López[1,5]

[1] Instituto de Bioingeniería, Universidad Miguel Hernández, E-03202 Elche, Spain
[2] Departamento de Ciencia de Materiales Óptica y Tecnología Electrónica, Universidad Miguel Hernández, E-03202 Elche, Spain
[3] Departament d'Optica i Optometria i Ciencies de la Visió, Universitat de València, E-46100 Burjassot, Spain
[4] Grupo de Investigación en Aplicaciones del Láser y Fotónica, Departamento de Física Aplicada, Universidad de Salamanca, E-37008 Salamanca, Spain
[5] Departamento de Física Aplicada, Universidad Miguel Hernández, E-03202 Elche, Spain
[*] Author to whom any correspondence should be addressed.

E-mail: pascuala.garcia@uv.es

Keywords: achromatic Fourier optics, geometric-phase lenses, supercontinuum laser illumination, broadband optical systems, ABCD matrix formalism, polarization-controlled systems, diffractive optics

OPEN ACCESS

RECEIVED
31 July 2025

REVISED
17 September 2025

ACCEPTED FOR PUBLICATION
25 September 2025

PUBLISHED
8 October 2025

Abstract

In this work we present a new configuration to achieve an achromatic all-optical Fourier transform (FT) using two blazed diffractive lenses and one non-dispersive lens. Different configurations are identified by imposing constraints on the ray matrix of the optical system, minimizing the wavelength dependence of both the transversal location of the FT plane and the FT spatial scaling. Experimental verification is carried out using geometric-phase (GP) flat diffractive lenses and an achromatic refractive lens. Furthermore, one identified novel configuration is symmetric. This symmetric triplet configuration enables a straightforward implementation in a reflective geometry that reduces the number of elements to a single GP lens combined with a mirror, thus leading to a highly-compact implementation. Experimental results are presented that validate the proposed systems.

1. Introduction

Fourier optics provides the fundamental theoretical framework for understanding and manipulating structured light [1]. A basic tool consists in performing the optical Fourier transform (FT) of the light field generated by a diffractive optical element (DOE) in the back focal plane of a positive lens [2]. However, when the DOE is illuminated with different wavelengths, the FT transform appears with a characteristic dispersion. Typically, singlet refractive lenses present chromatic aberration caused by the dispersion of the refractive index, which causes the lens focal length to depend on the wavelength. This aberration is typically corrected by building doublet (achromatic) or triplet (apochromatic) lenses in which two or more optical elements made of glasses with different dispersion properties are combined to bring two or three wavelengths to a common focus. Thus, in practice, non-dispersive refractive lenses can be built where the focal length can be considered constant in a wide spectral range [3], as it is the case of achromats and apochromatic lenses. While such designs greatly reduce chromatic aberrations in imaging systems, they do not eliminate the intrinsic wavelength dependence of the FT itself, because the scale of an optical FT is proportional to the product λf. Therefore, a thin lens with an ideal constant focal length provides an optical FT in a fixed plane for all wavelengths, but its size scales with wavelength. Namely, the longer the wavelength the bigger the size of the optical FT. If the DOE is located a distance from the lens equal to the focal length (i.e. it is located at the lens front focal plane) and it is illuminated with a collimated beam, an exact optical FT is obtained. If this is not the case, a quadratic phase factor arises which also depends on the wavelength. This phase factor is not relevant when only the intensity of the FT is of interest.

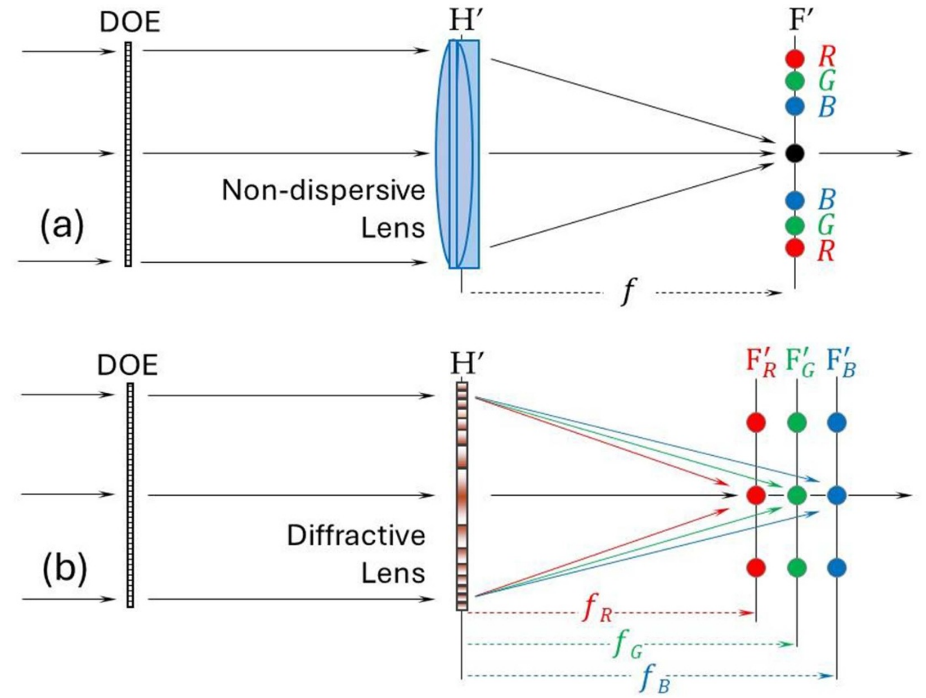

Figure 1. Illustration of the FT dispersion properties of a single lens: (a) a non-dispersive lens provides a common FT plane but a wavelength-dependent scaling. (b) a diffractive lens provides a constant scale, but the FT plane appears dispersed longitudinally. DOE: diffractive optical element, F′ indicates the lens back focal plane and H′ indicates the back principal plane, here located on the lens plane and assuming a thin lens.

Diffractive lenses represent a widespread alternative approach to perform the optical FT, with well-established fabrication technologies [4]. In a classical blazed diffractive lens, longer wavelengths are diffracted at larger angles resulting in shorter focal lengths, in a way that the product λf remains constant (or equivalently $P\sigma$ remains constant, where $P = 1/f$ is the lens optical power and $\sigma = 1/\lambda$) [5]. Therefore, diffractive lenses perform optical FT with the same scale for all wavelengths, but now the optical FT is focused on a different axial plane for each wavelength. In addition, only one wavelength can fulfill the exact FT condition since the DOE is placed at the lens front focal plane, thus for the rest of wavelengths there is an additional quadratic phase factor. Figure 1 illustrates these two properties of the optical FT obtained with a non-dispersive lens and with a diffractive lens.

Achromatic diffractive lenses have been demonstrated in liquid-crystal spatial light modulators [6], highlighting the important property of being reconfigurable. More recently, metalenses [7] and geometric-phase (GP) lenses [8] provided new ultra-thin lenses with achromatic focal length. All these designs are very useful in imaging applications [8] and ophthalmic optics [9] where chromatic aberration must be compensated. But if these lenses are used for obtaining an optical FT, the situation is equivalent to that provided by an ideal non-dispersive lens, i.e. the FT appears on the same plane for all wavelengths, but with a different scale.

The compensation of the dispersion properties to achieve a broadband achromatic optical FT was achieved by designing hybrid lens systems that cascade properly-separated diffractive and refractive lenses. In [10], a diffractive lens in-between two achromatic refractive lenses brings to the same output plane the longitudinally dispersed diffracted patterns generated by another diffractive lens, effectively leading to an achromatic diffraction pattern with a four-lens system (two diffractive lenses and two refractive lenses). Alternatively, a diffractive doublet illuminated with a converging beam having the same focus for all wavelengths (thus requiring a previous non-dispersive lens) was demonstrated in [11, 12].

In this work, we bring this latter approach forward and apply the ray matrix formalism to devise a new triplet-lens system that is highly advantageous in terms of simplicity and compactness. In contrast to [11, 12], it achieves achromatic performance with a simpler architecture: two diffractive lenses of equal focal length and opposite sign, placed at the extremes of the system, and one central equidistant non-dispersive lens of the same focal length. The experimental realization of such symmetric triplet-lens system is demonstrated using two GP lenses, acting as the diffractive lenses, and one achromatic refractive lens. The symmetry of this novel configuration enables a compact implementation in a reflective geometry that reduces the number of elements to a single GP lens combined with a mirror. This not only enhances experimental simplicity but also opens the door to highly compact designs.

The manuscript is organized as follows: after this introduction, section 2 presents the formal analysis based on the ray matrix formalism, where the conditions for achieving the achromatic FT and its different solutions for a triplet-lens system are derived, including the solution reported in [11, 12]. Section 3 focuses on the configuration we refer to as the symmetric triplet, whose experimental realization is demonstrated in section 4. Section 5 introduces the compact reflective variation of the symmetric triplet system and, finally, the conclusions of the work are provided in section 6.

2. Achromatic FT lens systems

Figure 2 illustrates the approach. We use the ray matrix (*ABCD* matrix) formalism to describe a compound lens system. This mathematical framework is widely used to analyze ray propagation in optical systems [13], and it is also very useful to analyze diffractive systems [14], including achromatic FT configurations [15]. The two basic building blocks are the free space propagation and the thin lens, represented respectively by the ray matrices $\mathbf{M}_P$ and $\mathbf{M}_L$ given by:

$$\mathbf{M}_P(d) = \begin{bmatrix} 1 & d \\ 0 & 1 \end{bmatrix}, \mathbf{M}_L(f) = \begin{bmatrix} 1 & 0 \\ -P & 1 \end{bmatrix}, \quad (1)$$

where d and $P = 1/f$ denote, respectively, the propagation distance and the lens power, f being the lens focal length. When a lens system is built by cascading multiple lenses separated by free-space propagations, the overall system is described by the ray matrix resulting from multiplying the individual elemental matrices. This overall matrix takes the general form

$$\mathbf{M}_S = \begin{bmatrix} A_S & B_S \\ C_S & D_S \end{bmatrix}, \quad (2)$$

where $\det[\mathbf{M}_S] = A_S D_S - C_S B_S = 1$.

Two parameters of the ray matrix are of relevance in this work. First, the parameter C_S is directly related to the system's focal length and optical power as $P_S = 1/f_S = -C_S$ [16]. Second, it is necessary to determine the location of the system's back focal plane (F′), where the optical FT is obtained. Therefore, a new free propagation of distance z is added to the system, yielding a new ray matrix:

$$\mathbf{M}_P(z) \times \mathbf{M}_S = \begin{bmatrix} 1 & z \\ 0 & 1 \end{bmatrix} \times \begin{bmatrix} A_S & B_S \\ C_S & D_S \end{bmatrix} = \begin{bmatrix} A_S + zC_S & B_S + zD_S \\ C_S & D_S \end{bmatrix}. \quad (3)$$

The condition for having F′ at the output requires that the A element of the resulting new ray matrix must be zero [17]. Thus, $A_S + zC_S = 0$ leads to the condition $z = -A_S/C_S$ to locate F′.

Thus, the following two ideal conditions must be imposed on the general compound system shown in figure 2 to achieve an achromatic optical FT system:

1) **Condition for constant scaling of the FT:** the compound system must exhibit a wavelength dependence of its focal length f_S such that the product λf_S remains constant (or equivalently the ratio $P_S\sigma$ is constant), and
2) **Condition for a constant plane of the FT**: all wavelengths must focus on a common back focal plane F′, which must be real to be physically accessible (i.e. the distance $z = -A_S/C_S$ must be positive).

Since the back focal plane F′ must be the same for all wavelengths, these conditions imply that the system's back principal plane H′ must change with the wavelength, the shorter the wavelength, the greater the distance to F′ (see figure 2(a)).

To fulfill these two conditions, the compound lens system must be composed of lenses with different chromatic dispersion properties. We consider ideal thin lenses that are either: (a) non-dispersive, whose focal length is assumed constant with wavelength (P does not change with $\xi \equiv \lambda/\lambda_0 = \sigma_0/\sigma$), or (b) classical blazed diffractive lenses, which typically exhibit an optical power that changes with wavelength as $P(\xi) = \xi P_0$, where P_0 represents the power for a reference wavelength $\lambda_0 = 1/\sigma_0$. For the sake of clarity, we use the same drawings as in figure 1 along the manuscript to describe the non-dispersive lenses and the diffractive lenses. Also, we will henceforth refer to the non-dispersive lenses simply as 'achromatic' lenses, although this term strictly refers to the achromatic doublet that brings two wavelengths to the same focal plane and has a reduced (but not flat) wavelength dispersion between those two wavelengths.

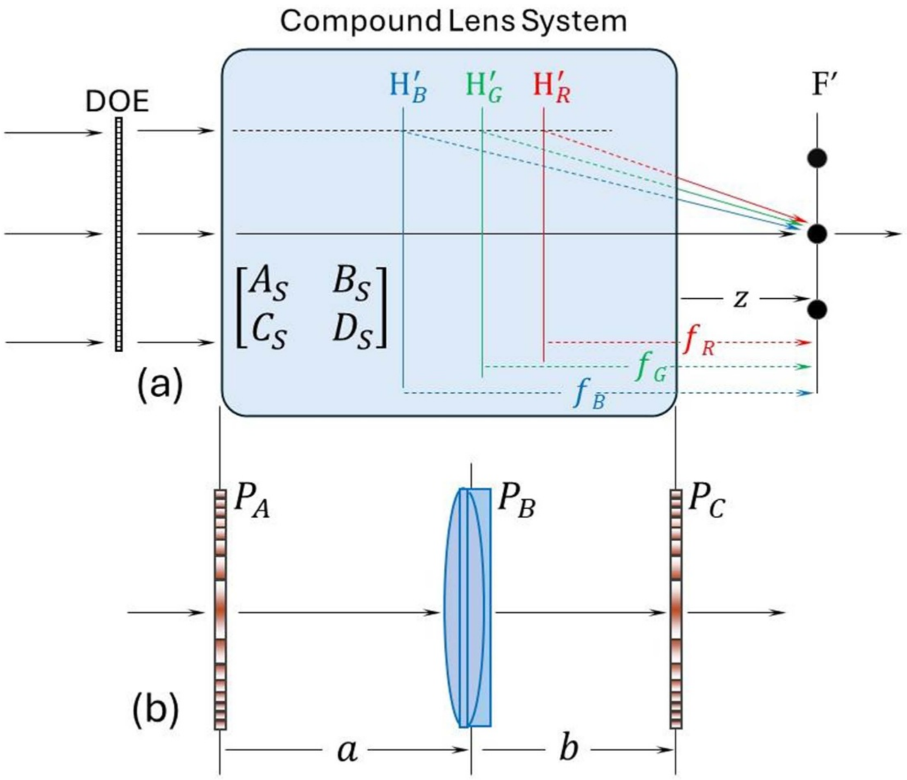

Figure 2. (a) Design of an achromatic FT system: a compound lens system described by its ray matrix is designed to have a back focal plane F′ common to all wavelengths and a focal length $f(\lambda)$ that changes with wavelength such that λf remains constant. The distance from the output surface to the back focal plane is indicated as z. (b) Scheme of a possible triplet system with a non-dispersive lens between two diffractive lenses.

The two above-mentioned conditions for achieving an achromatic FT cannot be satisfied using only two lenses. Thus, we directly consider a system composed of three lenses (figure 2(b)), with optical powers $P_A = 1/f_A$, $P_B = 1/f_B$ and $P_C = 1/f_C$ respectively, separated by distances a and b. The ray matrix for this triplet is calculated as:

$$\mathbf{M}_S = \begin{bmatrix} 1 & 0 \\ -P_C & 1 \end{bmatrix} \times \begin{bmatrix} 1 & b \\ 0 & 1 \end{bmatrix} \times \begin{bmatrix} 1 & 0 \\ -P_B & 1 \end{bmatrix} \times \begin{bmatrix} 1 & a \\ 0 & 1 \end{bmatrix} \times \begin{bmatrix} 1 & 0 \\ -P_A & 1 \end{bmatrix}, \tag{4}$$

which yields the following general matrix:

$$\mathbf{M}_S = \begin{bmatrix} 1-(a+b)P_A - bP_B + abP_AP_B & a+b-abP_B \\ C_S & 1-(a+b)P_C - aP_B + abP_BP_C \end{bmatrix}. \tag{5}$$

Parameter C_S in equation (5) gives the optical power $P_S = -C_S$ of the triplet system, which is given by:

$$P_S = P_A + P_B + P_C - (a+b)P_AP_C - aP_AP_B - bP_BP_C + abP_AP_BP_C. \tag{6}$$

Parameter A_S, together with the optical power P_S, provides the distance $z = -A_S/C_S$ to the system's back focal plane F′ as

$$z = \frac{A_S}{P_S} = \frac{1-(a+b)P_A - bP_B + abP_AP_B}{P_S}. \tag{7}$$

Equations (6) and (7) provide the solution to find the configurations leading to an achromatic FT triplet-lens system. Five parameters (three focal lengths and two inter-lens distances) can be set to meet the required constraints.

The two constraints described above, expressed in terms of the triplet system optical power P_S and the distance z, can be written as:

1) **Condition for constant scaling of the FT:** the compound system must exhibit a power dependence $P_S(\xi) = \xi P_{S0}$ where P_{S0} is the triplet optical power for the reference wavelength ($\xi = 1$). This condition can be written as

$$\frac{\mathrm{d}}{\mathrm{d}\xi}\left[\frac{P_S(\xi)}{\xi}\right] = 0 \tag{8}$$

2) **Condition for a constant plane of the FT**: the distance $z(\xi)$ must remain constant for all wavelengths, i.e.:

$$\frac{\mathrm{d}z(\xi)}{\mathrm{d}\xi} = 0. \tag{9}$$

Since $z(\xi) = A_S(\xi)/P_S(\xi)$, equation (9) can be rewritten as

$$\frac{\mathrm{d}A_S(\xi)}{\mathrm{d}\xi}P_S(\xi) - A_S(\xi)\frac{\mathrm{d}P_S(\xi)}{\mathrm{d}\xi} = 0. \tag{10}$$

On the other hand, note that equation (8) can be alternatively written as:

$$\xi\frac{\mathrm{d}P_S(\xi)}{\mathrm{d}\xi} - P_S(\xi) = 0. \tag{11}$$

Hence $\mathrm{d}P_S(\xi)/\mathrm{d}\xi = P_S(\xi)/\xi$, which applied to equation (10) yields the following relation:

$$\xi\frac{\mathrm{d}A_S(\xi)}{\mathrm{d}\xi} - A_S(\xi) = 0. \tag{12}$$

Equations (11) and (12) share the same mathematical form, and they represent the ideal conditions of the ray matrix required to achieve an achromatic FT. However, as will be shown next, these two conditions cannot be fulfilled simultaneously for all wavelengths. Therefore, following the approach of Lancis *et al* in [11], we take a first-order approximation where the differential equations are considered exact for the reference value λ_0 ($\xi = 1$), i.e.

$$\left(\xi\frac{\mathrm{d}P_S(\xi)}{\mathrm{d}\xi} - P_S(\xi)\right)\Bigg|_{\xi=1} = 0, \quad \left(\xi\frac{\mathrm{d}A_S(\xi)}{\mathrm{d}\xi} - A_S(\xi)\right)\Bigg|_{\xi=1} = 0. \tag{13}$$

Next, it is shown that different solutions to these equations can be obtained using a triplet-lens system, in which we consider two of the lenses diffractive and an achromatic refractive lens. In the following, we discuss two possible designs depending on the position of the achromatic lens.

2.1. System 1: Achromat followed by a separated diffractive doublet

Figure 3(a) represents a first possible triplet design, where the first lens is an achromatic refractive lens followed by a diffractive doublet, equivalent to the design proposed in [11]. The optical power of the first lens $P_A(\xi) = P_{A0}$ is constant, but P_B and P_C change with wavelength as $P_{B/C}(\xi) = \xi P_{B0/C0}$, with P_{A0}, P_{B0} and P_{C0} denoting the power of each lens at the reference wavelength λ_0 ($\xi = 1$). Thus, the triplet optical power, given by equation (6), reads:

$$P_S(\xi) = P_{A0} + \xi P_{B0} + \xi P_{C0} - \xi(a+b)P_{A0}P_{C0} - \xi aP_{A0}P_{B0} - \xi^2 bP_{B0}P_{C0} + \xi^2 abP_{A0}P_{B0}P_{C0} \tag{14}$$

Therefore, by inserting this function $P_S(\xi)$ into equation (11), the following relation is obtained:

$$P_{A0} + bP_{B0}P_{C0}\xi^2 - abP_{A0}P_{B0}P_{C0}\xi^2 = 0. \tag{15}$$

Similarly, the matrix element $A_S(\xi)$ in equation (5) is then given by

$$A_S(\xi) = 1 - (a+b)P_{A0} - bP_{B0}\xi + abP_{A0}P_{B0}\xi, \tag{16}$$

and equation (12) leads to

$$P_{A0} = \frac{1}{a+b}. \tag{17}$$

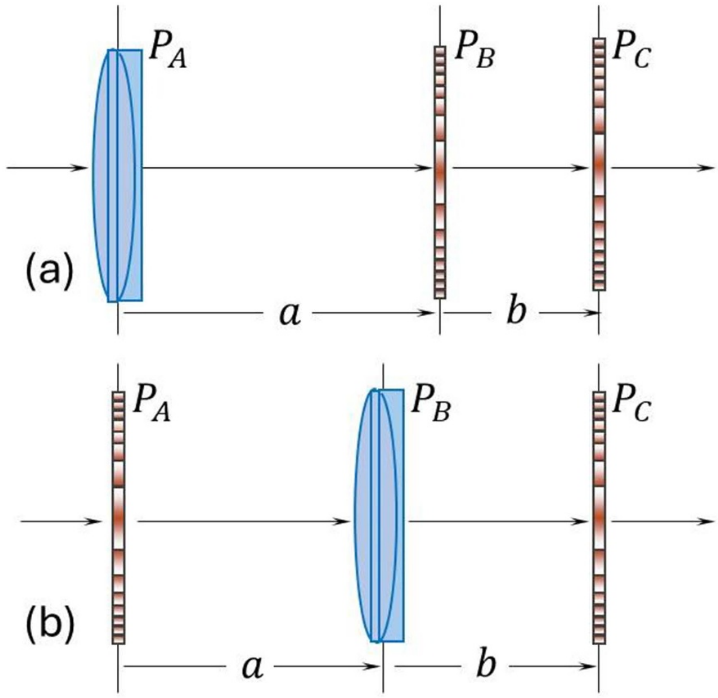

Figure 3. Possible configurations for the achromatic FT system. A collimated input beam is considered in all cases. (a) Non-dispersive lens followed by a separate diffractive doublet. (b) Non-dispersive lens between two diffractive lenses.

Now, considering this relation into equation (15), the following expression is obtained for the distance b between the second and the third lens:

$$b^2 = \frac{-1}{\xi^2 P_{B0} P_{C0}}. \tag{18}$$

Equations (17) and (18) provide the solution to achieve an achromatic FT system. Note that equation (17) does not depend on $\xi = \lambda/\lambda_0$ meaning that it can be fulfilled for all wavelengths. It also reveals that the focal length of the first lens must satisfy $f_{A0} = a + b$. Therefore, a collimated input beam is focused by this lens to the plane where the third lens is placed. The relation in equation (18) depends on ξ, meaning that it cannot be accomplished by all wavelengths. As mentioned, we approximate the relations around the reference value $\xi = 1$, so equation (18) can be rewritten as $b = \sqrt{-f_{B0} f_{C0}}$. This implies that the two diffractive lenses must have opposite signs, one being converging and the other diverging. The above conditions exactly reproduce the system originally proposed by Lancis *et al* in [11].

2.2. System 2: Achromat between diffractive lenses

In this work we propose a second possible triplet design, depicted in figure 3(b) that also enables the realization of an achromatic FT. As it will be discussed, it allows to be implemented as a compact and simple system. In this design the non-dispersive lens is placed between two diffractive lenses. Accordingly, the optical power of the central lens is constant $P_B(\xi) = P_{B0}$, while the optical powers of the first and third lenses are $P_{A/C}(\xi) = \xi P_{A0/C0}$. Thus, the triplet optical power given by equation (6) is now

$$P_S(\xi) = \xi P_{A0} + P_{B0} + \xi P_{C0} - \xi^2 (a+b) P_{A0} P_{C0} - \xi a P_{A0} P_{B0} - \xi b P_{B0} P_{C0} + \xi^2 ab P_{A0} P_{B0} P_{C0}. \tag{19}$$

Therefore, equation (11) leads to the relation:

$$P_{B0} + P_{A0} P_{C0} (a + b - ab P_{B0}) \xi^2 = 0. \tag{20}$$

In addition, parameter $A_S(\xi)$ of the general matrix in equation (5) now reads

$$A_S(\xi) = 1 - (a+b) P_{A0} \xi - b P_{B0} + ab P_{A0} P_{B0} \xi, . \tag{21}$$

And consequently equation (12) leads to

$$P_{B0} = \frac{1}{b}, \tag{22}$$

i.e. the distance between the second and the third lens must be set equal to the focal length of the second lens, $b = f_{B0}$.

Hence, inserting equation (22) in equation (20), the following relation between the powers of the three lenses is obtained: $P_{B0}^2 = -\xi^2 P_{A0} P_{C0}$. Since this relation depends on ξ, it cannot be fulfilled for all wavelengths. Thus, once again we consider the first-order approximation by taking it at the reference wavelength, $\xi = \lambda/\lambda_0 = 1$, leading to:

$$P_{B0}^2 = -P_{A0} P_{C0}, \tag{23}$$

which, written in terms of the focal length yields $f_{B0}^2 = -f_{A0} f_{C0}$. This relation reveals that the first and third lens must have opposite signs, one converging and one diverging. Equations (22) and (23) provide the solution required to achieve the achromatic FT system with the configuration depicted in figure 3(b). When setting the system's parameters (three focal lengths and two inter-lens distances), it is worth noting that besides fulfilling equations (22) and (23) an implicit third condition must be fulfilled: the parameters must ensure a real FT plane (positive z in equation (7)). This is also the case of the configuration in figure 3(a), with derived conditions equations (17) and (18). Therefore, both configurations have in principle two degrees of freedom and different possible solutions. Obviously, they will all feature residual chromatic aberration, since in both cases the first-order approximation was considered in deriving the condition equations (namely, equation (23) and equation (18)).

3. The symmetric triplet configuration

The first system was experimentally verified in previous works [12, 15]. Thus, here we present the experimental verification of the second configuration which, in turn, admits various solutions. Among them, one is particularly simple and practical; we call it the symmetric triplet. It arises when the two diffractive lenses have equal optical powers but with opposite sign, and the first one is selected as the diverging lens, i.e. $P_{A0} = -P_{C0} = -1/f$. In this situation, equation (23) leads to $P_{B0} = 1/f$, i.e. the achromatic lens must be positive with the same focal length f. Additionally, from equation (22) follows that $b = f$. Finally, we choose the remaining distance a (which is a free parameter) to be $a = f$. Introducing these parameters into equations (6) and (7), the triplet optical power at the reference wavelength is $P_{S0} = 2/f$ and the distance from the last lens to the triplet back focal plane F′ (where the achromatic FT is focused) is $z = f/2$. This positive value ensures that the FT appears in an accessible real plane. Thus, such configuration, where all distances are the same, is very convenient in terms of simplicity and compactness, as will be shown in the next section.

This symmetric triplet is sketched in figure 4, together with the ray trajectories for an input collimated beam. Green rays (indicated as G in the figure) represent the reference wavelength (λ_0), which typically corresponds to the center of the spectral band. In this situation, the first diffractive lens (Lens A) makes the beam diverge, giving a virtual focus O_G a distance f left to the lens. The achromatic lens (Lens B), which lays a distance $2f$ from this virtual focus, then converges the beam to an image point O'_G located $2f$ behind Lens B. Finally, the second diffractive lens (Lens C) further converges the beam, forming the FT at a distance $f/2$ behind Lens C. Intuitively, the symmetric triplet balances the opposite chromatic trends introduced by the two diffractive lenses, so that the wavelength-dependent shifts are compensated to first order, leaving only a small residual aberration.

The rays drawn as red lines in figure 4 (indicated as R) represent a longer wavelength and illustrate how the triplet system maintains the achromatic performance. Due to the diffractive nature of Lens A, the red beam is diffracted at a larger angle than the green beam, producing a virtual focus O_R located closer to the lens. Therefore, the achromatic Lens B provides an image point O'_R located beyond O'_G. When the beam impinges on Lens C (the last diffractive lens) again the red beam is diffracted at a larger angle than the green beam, such that both wavelengths converge towards the same output plane. For wavelengths shorter than the reference one, the diffraction angles produced by Lenses A and C are smaller, and the locations of the corresponding points O and O′ are just the opposite with respect to O_G and O'_G, again leading to the achromatic final spot F′. In fact, as explained in [11], the beam impinging on the last diffractive lens can be viewed as forming a frustum of a cone, that forms the achromatic final image.

The triplet lens FT system exhibits a residual chromatic aberration, both in the transverse and longitudinal directions. Since the FT scale is proportional to the product $\lambda f_S(\lambda)$, the transverse chromatic aberration (TCA) can be defined as the ratio between the relative variation of this product over the spectral range compared to its value at the central reference wavelength:

$$\mathrm{TCA} = \frac{\lambda_0 f_{S0} - \lambda f_S(\lambda)}{\lambda_0 f_{S0}} = 1 - \frac{\xi P_{S0}}{P_S(\xi)}. \tag{24}$$

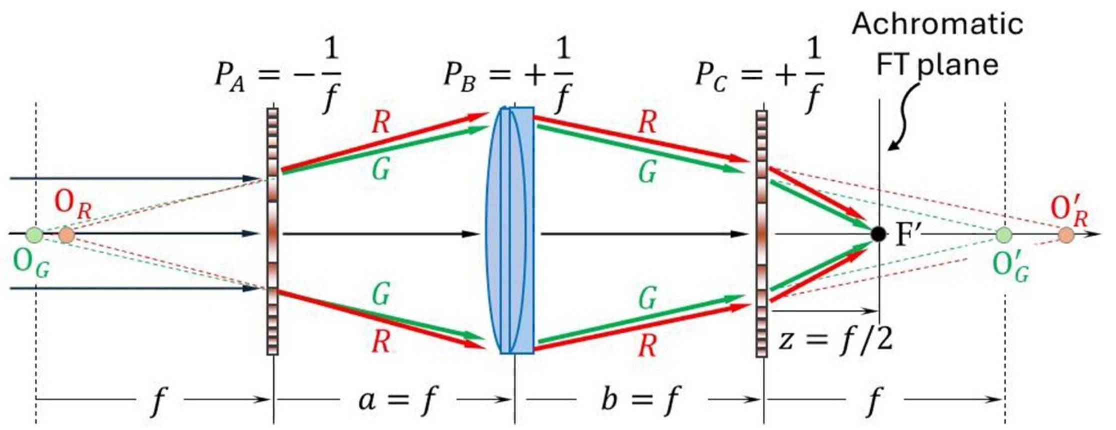

Figure 4. Scheme of the symmetric achromatic FT triplet lens system: Lens A is a negative diffractive lens with focal length $-f$, followed by an achromatic lens (Lens B) of focal length $+f$ separated a distance $a = f$, and another diffractive lens (Lens C) with focal length $+f$ separated a distance $b = f$. The FT plane appears at a distance $z = +f/2$ from Lens C and the effective focal length of the triplet lens is $f/2$ for the reference wavelength.

Similarly, the longitudinal chromatic aberration (LCA) can be defined as the ratio between the variation of $z(\xi)$ over the spectral range with respect to the reference wavelength, i.e:

$$\mathrm{LCA} = \frac{z(\lambda_0) - z(\lambda)}{z(\lambda_0)}. \tag{25}$$

The chromatic aberrations of the triplet system are due to the individual lenses. The achromatic lens causes TCA while the diffracted lenses cause LCA, as clearly illustrated in figure 1. Hence, it is relevant to compare the TCA and LCA of the triplet system with that of an individual achromatic and diffractive lens of equivalent focal length. Thus, figure 5 shows the functions TCA(λ) and LCA(λ) covering the visible spectral range for a symmetric triplet-lens system with $f = 100$ mm and reference wavelength $\lambda_0 = 550$ nm. For comparison, figure 5(a) includes the TCA for an ideal achromatic lens of 50 mm focal length (thus equivalent to the triplet-lens system focal length $f/2 = 50$ mm at the reference wavelength), while figure 5(b) shows the corresponding LCA for a diffractive lens with 50 mm focal length at the reference wavelength. As it is observed, both TCA(λ) and LCA(λ) exhibit a reduced wavelength variation for the proposed triplet-lens system, namely less than 6% in the 400–700 nm wavelength range.

This figure also includes the TCA(λ) and LCA(λ) curves for the configuration in figure 3(a), which is equivalent to the design proposed by Lancis *et al* in [11] and was described in section 2.1. These curves are calculated considering a first achromatic lens with focal length $f_A = +75$ mm, followed by two diffractive lenses with focal lengths $f_B = -100$ mm and $f_C = +25$ mm at the reference wavelength. By setting the inter-lens distances as $a = 25$ mm and $b = 50$ mm, the conditions given in equations (17) and (18) are satisfied and the system's focal length becomes also $f_S = +50$ mm. This allows a direct comparison of the chromatic aberration performance of both triplet designs. As shown, the proposed symmetric triplet exhibits average TCA and LCA values below 1.34% in the 400–700 nm spectral range, with a slightly better performance than Lancis's triplet system, which shows TCA and LCA averaged values above 1.76% in the same spectral range.

4. Experimental implementation with geometric phase lenses

We have experimentally verified this symmetric triplet achromatic lens system using two GP lenses and one achromatic refractive lens. GP lenses are modern flat diffractive kinoform lenses consisting in micro-structured half-wave retarders where the lens phase function is encoded on the spatial distribution of the retarder's optical axis. Therefore, a GP lens behaves as a converging lens for one circular polarization and as a diverging lens with the same focal length but opposite sign for the orthogonal circular polarization [18]. Two GP lenses acquired from Edmund Optics (polarization-directed flat lenses, discontinued model #34-466) are employed. They consist of polymerized liquid-crystal thin-films, approximately 0.45 mm thick, with 2.5×2.5 cm^2 effective area and 100 mm nominal focal length. Although the half-wave retardance condition of the GP lens is exactly fulfilled only at the central wavelength of 550 nm, the liquid-crystal layer is a zero-order retarder, thus featuring a fairly flat retardance dispersion throughout the visible range. The

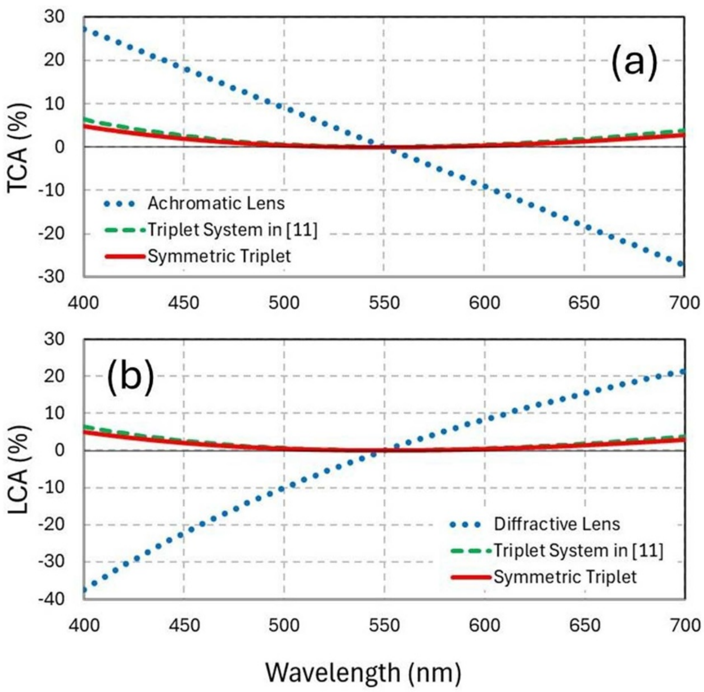

Figure 5. Chromatic aberration performance in the visible spectral range (400–700 nm) of the new proposed symmetric triplet-lens system (figure 4) and the triplet-lens system proposed by Lancis *et al* in [11] having equivalent focal length: (a) transversal chromatic aberration (TCA) in the FT plane compared with an achromatic lens of equivalent focal length. (b) Longitudinal chromatic aberration (LCA) in the FT plane compared with a diffractive lens of equivalent focal length. The reference wavelength is 550 nm.

small retardance mismatch at other wavelengths causes a small reduction of the polarization-conversion efficiency, which simply results in a weak background.

We built the triplet lens system in figure 4 with two such GP lenses and an achromatic refractive lens (Thorlabs, AC508-100-A) of also 100 mm focal length and nominal wavelength range 400–700 nm. The separation between lenses was 100 mm. The system was illuminated with a supercontinuum laser (Fianium, SC400). The laser was first polarized with a Glan–Taylor polarizing cube (Edmund Optics, #89-547 model) that provides a nominal extinction ratio below 5×10^{-5}over the spectral range between 50 and 2300 nm. An achromatic quarter-wave plate (Thorlabs, AQWP05M-600) was aligned to generate circularly polarized light across the visible spectrum.

The first GP lens was oriented such that it acts as a diverging lens on the input circular polarization (note that if the GP lens is flipped, it behaves as a converging lens for the same input circular polarization [19]). After passing through this first GP lens, the polarization state changes to the opposite circular polarization, which remains unaffected by the achromatic lens. Therefore, GP Lens 2 (placed in the same orientation as GP Lens 1) acts as a converging lens, thus completing the symmetric triplet configuration in figure 4. The optical FT appears 50 mm behind the GP Lens 2, where a diffuser is placed. As diffractive element we use the NEMO plastic card [20], which contains different DOEs. Figure 6(a) shows a photograph of the experimental setup. A color camera (Basler scA1390-17 fc, having 1390×1038 square pixels of 4.65 μm side) with an attached objective (Computer MLH 10X) captures the FT pattern.

It is worth noting that the symmetric triplet configuration can also be implemented with standard polarization-independent diffractive lenses (instead of GP lenses), in which case the input beam does not need to be circularly polarized. The use of planar GP lenses, though, offers the practical advantage of facilitating a precise adjustment of inter-lens distances.

In our experiments we employ three different DOEs: a grating generating orders in diagonal directions, and two computer-generated holograms designed to generate a flag and a rectangular grid in the FT plane. Figures 6(b)–(d) show the FT results obtained using a single GP lens. As expected, these FT patterns exhibit a significant dispersion. In contrast, figures 6(e)–(g) display the corresponding results obtained with the achromatic symmetric triplet-lens system. Now the diffraction orders appear white (figure 6(e)) and the holograms reproduce the FT pattern with slight chromatic dispersion (figures 6(f) and (g)). It is worth noting that the scale of the patterns in figures 6(e)–(g) is half of those in figures 6(b)–(d) since the triplet system has a 50 mm focal length, whereas the GP lens alone has a 100 mm focal length.

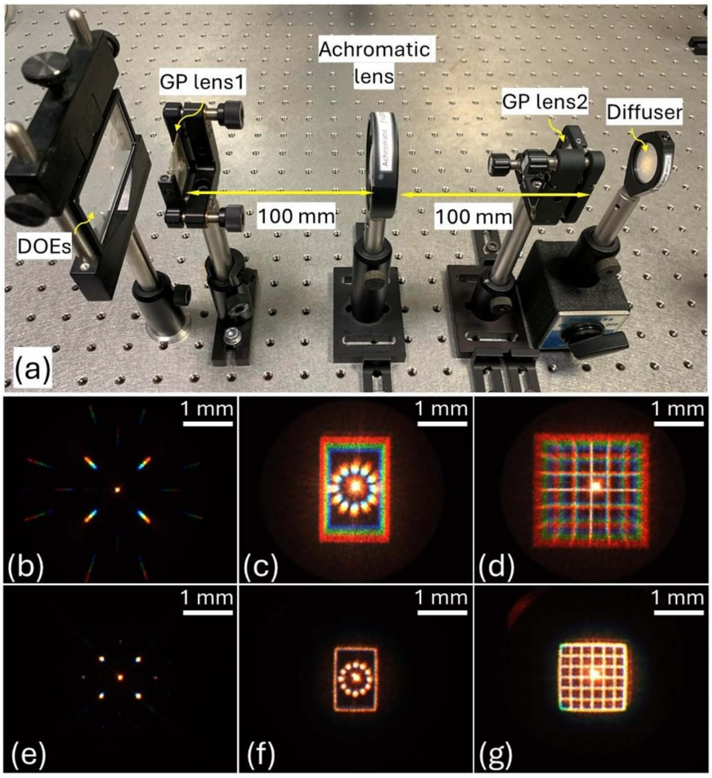

Figure 6. (a) Photograph of the experimental optical setup. Experimental results for the FT of three different DOEs obtained with ((b)–(d) a single GP lens, (e)–(g) the achromatic triplet-lens system.

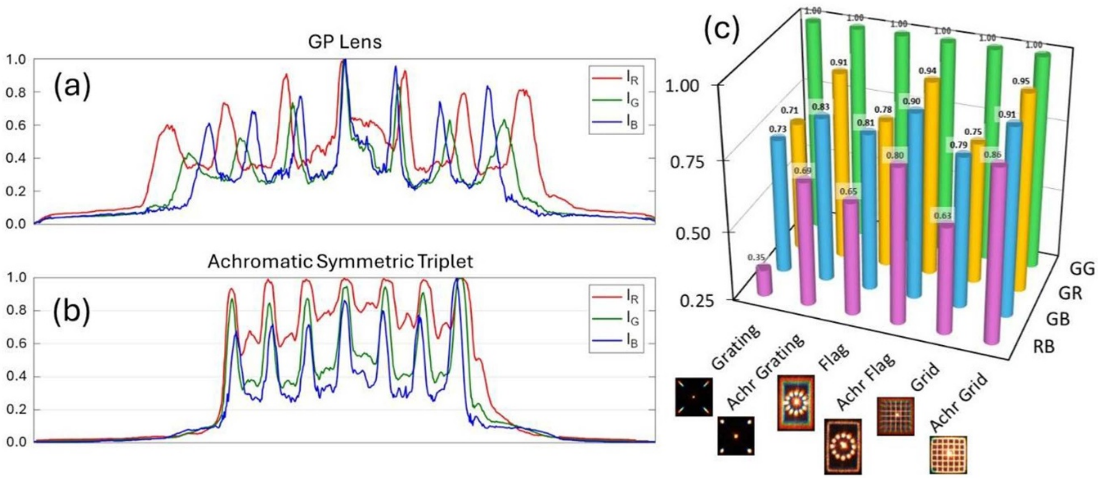

Figure 7. Intensity profiles along a horizontal line of the experimental FT obtained for the grid DOE with: (a) a single GP lens (figures 6(d)) and (b) the symmetric triplet (figure 6(g)). (c) Cross-correlation values obtained between the RGB channels of the experimental images in figures 6(b)–(g), normalized to the autocorrelation of the G channel.

In order to evaluate the degree of achromaticity achieved, the above experimental FT images were decomposed into their RGB components. Figures 7(a) and (b) show the intensity profiles in each color channel for the rectangular grid in figures 6(d) and (g), respectively, along a horizontal line. The achromatic correction is evident in figure 7(b), where the peaks of the three channels coincides, in contrast to the lateral shifts observed in figure 7(a).

In addition, we have evaluated the correlation between the RGB channels for each of the six experimental FT patterns shown in figures 6(b)–(g). The cross-correlation of the G–R, G–B and R–B channels of each image was calculated and normalized to the autocorrelation G–G of the green channel, taken as reference. These results are presented in figure 7(c), where 'Achr' denotes the FT pattern obtained with the achromatic triplet. The correlation values confirm the achromatic performance of the triplet-lens system with respect to

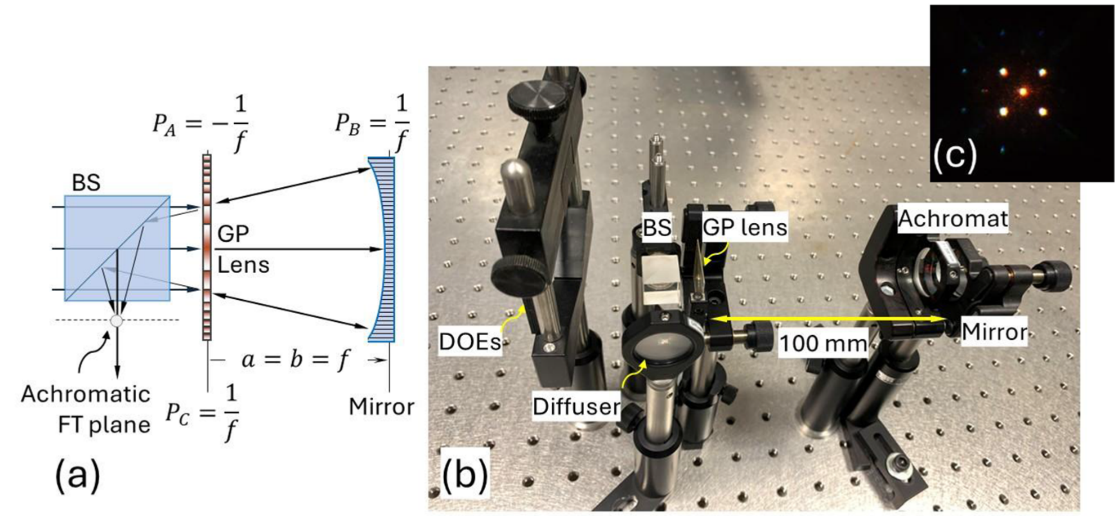

Figure 8. (a) Scheme of the reflective geometry for the achromatic system, using a beam splitter (BS) a GP lens and a converging mirror. (b) Photograph of the experimental optical setup, with $f = 100$mm. (c) Example of the achromatic FT obtained with a diffraction grating.

the single GP lens. In all three cases, the achromatic version exhibits a significantly higher correlation between color channels. The most notable improvement occurs for the grating, where the R–B correlation increases by more than 100%. In the cases of the flag and the grid DOEs, the R–B correlation increases by 23% and 36%, respectively. For the grid DOE, the cross-correlation between all channels remains above 86%.

5. The compact reflective symmetric triplet configuration

The above demonstrated symmetric triplet configuration is particularly advantageous because it can be easily implemented in a reflective geometry with a single GP lens, thus making the system more compact. GP lenses exhibit two key properties when illuminated with circularly polarized light: (1) after transmission through the GP lens, the polarization changes to the opposite circular polarization [18], and (2) the sign of the focal length depends on the direction of incidence—specifically, a GP lens behaves as a converging or diverging lens depending on the side from which the circularly polarized beam impinges [19]. Thus, if a circularly polarized input beam traversing the GP lens in the forward direction experiences a focal length $-f$, when the transmitted beam reflects back towards the GP lens, the beam propagating backwards experiences an opposite focal length $+f$. This property enables the construction of a compact symmetric achromatic triplet system.

Figure 8(a) shows a scheme of the proposed reflective geometry. Input circularly polarized light impinges on a GP lens with diverging focal length of -100 mm. The achromatic lens in figure 4 is now replaced with a spherical mirror of $+100$ mm focal length. In practice, we used an achromatic refractive lens of focal length $+200$ mm placed together with a flat mirror. Upon reflection, the beam now experiences a focal length of $+100$ mm in the backwards propagation through the GP lens. Finally, a beam splitter separates the output beam from the input path. Figure 8(b) shows a photograph of the experimental setup built in the laboratory. The DOEs card, placed just before the beam splitter, is illuminated with circularly polarized broadband light. A diffuser is located in the output path, at the FT plane, whose diffraction pattern is imaged onto the color camera. Figure 7(c) presents the achromatic FT obtained when using as DOE the same diffraction grating as the one in figure 6(e). The results are equivalent, confirming the effectiveness of this compact reflective system. Notably, the total length of the optical setup, from the DOE to the mirror, is less than 150 mm.

6. Conclusions

In summary, we have proposed and experimentally demonstrated a novel optical system to obtain achromatic optical FTs. Two ideal conditions are identified on the ABCD ray matrix of a lens system to ensure a wavelength-independent FT condition: equation (8) for achieving a constant scaling factor and equation (9) for achieving a single axial FT plane. Following previous approaches [11], we consider less restrictive conditions leading to an achromatic FT system which can be fulfilled by a triplet-lens system composed of one achromatic lens and two diffractive lenses.

While earlier works [11, 12] implemented the triplet system with the achromatic lens as the first element, followed by a diffractive doublet, here we introduce a different configuration where the non-dispersive lens is placed between the two diffractive lenses. We derive the conditions (equation (22) and (23)) to achieve the achromatic FT and propose a symmetric triplet-lens system that holds significant advantages. This system is experimentally validated using a supercontinuum laser source and (without loss of generality) employing GP lenses as the diffracted lenses. Furthermore, a compact reflective configuration is demonstrated, which leverages the unique polarization-dependent properties of GP lenses.

Although this proof-of-concept demonstration of the proposed system will require further optimizations, like including the aberrations of the optical components—mainly the GP lenses—as well as tolerances to imperfections in the system parameters—inter-lens distances—the proposed new configuration could be relevant for different applications. One possibility is within the field of ultrashort pulsed laser beams, where achromatic diffractive systems are required to minimize chromatic dispersion [21, 22]. The chromatic control and compensation could be further exploited in Fourier systems to generate structured spatio-temporal optical fields [23]. Also, the scalability of electromagnetic waves allows extending the proposed system to other spectral ranges of interest, including infrared light [24], for applications such as high-harmonics generation [25] and terahertz waves [26]. In all these cases, the rapid development of metasurface technology [27] offers a path to integrate more compact, scalable and even tunable achromatic optical systems.

Data availability statement

The data that support the findings of this study are available upon reasonable request from the authors.

Acknowledgment

We acknowledge financial support from Ministerio de Ciencia e Innovación, Spain (ref. PID2021-126509OB-C22 and PDC2022-133332-C22). S. Ríos-Álvarez acknowledges a grant from Generalitat Valenciana, Santiago Grisolia Program (ref. CIGRIS/2023/043).

Author contributions

Ignacio Moreno 0000-0002-1550-0601
Conceptualization (lead), Formal analysis (lead), Funding acquisition (lead), Investigation (lead), Resources (lead), Supervision (lead), Writing – original draft (lead), Writing – review & editing (equal)

Santiago Ríos-Álvarez 0000-0003-0375-1961
Formal analysis (supporting), Investigation (supporting), Software (supporting)

Pascuala García-Martínez 0000-0002-8537-281X
Conceptualization (equal), Formal analysis (lead), Funding acquisition (equal), Methodology (lead), Writing – original draft (equal), Writing – review & editing (lead)

David Marco 0000-0003-0039-4161
Conceptualization (equal), Formal analysis (equal), Investigation (equal), Writing – review & editing (equal)

María del Mar Sánchez-López 0000-0002-6286-0079
Formal analysis (lead), Funding acquisition (lead), Investigation (lead), Supervision (lead), Writing – original draft (equal), Writing – review & editing (lead)

References

[1] Rosales-Guzmán C, Perez-Garcia B and Cox M A 2024 The compact cookbook of structured modes of light *J. Phys.* **6** 043004
[2] Goodman J W 2017 *Introduction to Fourier Optics* 4th edn (W. H. Freeman)
[3] Malacara-Hernández D and Malacara-Hernández Z 2013 *Handbook of Optical Design* 3rd edn (CRC Press)
[4] Shi C, Zhao W, Chen S and Li W 2024 Multilevel diffractive lenses: recent advances and applications *Symmetry* **16** 1337
[5] De Wit J M M, Cussiol F, Caglayan H and Gómez Rivas J 2025 Diffraction and dispersion effects on the wavelength dependence of the focal length of metalenses *Appl. Opt.* **64** 3598–604
[6] Márquez A, Iemmi C, Campos J and Yzuel M J 2006 Achromatic diffractive lens written onto a liquid crystal display *Opt. Lett.* **31** 392–4
[7] Khorasaninejad M, Chen W T, Zhu A Y, Oh J, Devlin R C, Roques-Carmes C, Mishra I and Capasso F 2017 Visible wavelength planar metalenses based on titanium dioxide *IEEE J. Sel. Top. Quantum Electron.* **23** 4700216
[8] Luo Z, Li Y, Rao Y and Wu S-T 2023 Achromatic diffractive liquid-crystal optics for virtual reality displays *Light Sci. Appl.* **12** 230
[9] Clavé L, Faria-Ribeiro M and Millan M S 2024 Chromatic changes in vision with diffractive ophthalmic optics *Opt. Express* **32** 10348–61

[10] Ferriere R and Goedgebuer J P 1983 Achromatic system for far-field diffraction with broadband illumination *Appl. Opt.* **22** 1540–5
[11] Lancis J, Andrés P, Furlan W D and Pons A 1994 All-diffractive achromatic Fourier-transform setup *Opt. Lett.* **19** 402–4
[12] Tajahuerce E, Climent V, Lancis J, Fernández-Alonso M and Andrés P 1998 Achromatic Fourier transforming properties of a separated diffractive lens doublet: theory and experiment *Appl. Opt.* **37** 6164–73
[13] Kloos G 2007 *Matrix Methods for Optical Layout* (SPIE, Bellingham)
[14] Davis J A and Lilly R A 1993 Ray-matrix approach for diffractive optics *Appl. Opt.* **32** 155–8
[15] Lancis J, Mínguez-Vega G, Tajahuerce E, Climent V, Andrés P and Caraquitena J 2004 Chromatic compensation of broadband light diffraction: ABCD-matrix approach *J. Opt. Soc. Am. A* **21** 1875–85
[16] Moreno I and Ferreira C 2010 Fractional Fourier transforms and geometrical optics *Advances in Imaging and Electron Physics* vol 161 (Academic Press) ch 3,pp 89–146
[17] Moreno I, Sánchez-López M M, Ferreira C, Davis J A and Mateos F 2005 Teaching Fourier optics through ray matrices *Eur. J. Phys.* **26** 261–71
[18] Zhan T, Xiong J, Lee Y-H and Wu S-T 2017 Polarization-independent Pancharatnam-Berry phase lens system *Opt. Express* **26** 35026–33
[19] García-Martínez P and Moreno I 2023 Dual polarization Fourier transform processor using geometric-phase lenses *Opt. Express* **31** 16460–70
[20] Thienpont H, Mohr J, Kujawinska M, Taghizadeh M R, Waddie A J, Mappes T, Wyrowski F and Stijns E 2007 The NEMO educational kit *Proc. SPIE* **9665** 96651S
[21] Mínguez-Vega G, Lancis J, Caraquitena J, Torres-Company V and Andrés P 2006 High spatiotemporal resolution in multifocal processing with femtosecond laser pulses *Opt. Lett.* **31** 2631–3
[22] Amako J and Nakano H 2021 Achromatic optical system with diffractive-refractive hybrid lenses for multifocusing of ultrashort pulse beams *Opt. Express* **29** 4488–503
[23] Yessenov M and Abouraddy A F 2025 Optical spatiotemporal Fourier synthesis: tutorial *J. Opt. Soc. Am. A* **42** 1295–315
[24] Zhang Y *et al* 2024 Advances and challenges of ultrafast fiber lasers in 2–4 μm mid-infrared spectral regions *Lasers Photon. Rev.* **18** 2300786
[25] Alonso B, Lopez-Quintas I, Holgado W, Drevinskas R, Kazansky P, Hernández-García C and Sola I 2020 Complete spatiotemporal and polarization characterization of ultrafast vector beams *Commun. Phys.* **3** 151
[26] Du Y, Feng H and Wu S 2024 Synthetic aperture imaging with pulsed terahertz waves and its application in three-dimensional modeling of complex structures *Appl. Phys. B* **130** 2012
[27] Kim J, Seong J, Yang Y, Moon S-W, Badloe T and Rho J 2022 Tunable metasurfaces towards versatile metalenses and metaholograms: a review *Adv. Photon.* **4** 024001